Disk Micelles from Nonionic Coil−Coil Diblock Copolymers

William F. Edmonds,[†] Zhibo Li,[‡] Marc A. Hillmyer,[‡] and Timothy P. Lodge*[,†,‡]

Department of Chemical Engineering and Materials Science and Department of Chemistry, University of Minnesota, Minneapolis, Minnesota 55455

Received March 21, 2006; Revised Manuscript Received April 25, 2006

ABSTRACT: The micellization of an almost symmetric diblock copolymer, 1,2-polybutadiene-*b*-poly(hexafluoropropylene oxide), with block molecular weights of 6000 and 5700, respectively, was examined in the polybutadiene-selective solvent bis(2-ethylhexyl) phthalate. Cryogenic transmission electron microscopy indicated that the copolymer self-assembled into thin disk micelles, with radii from 20 to 150 nm. Small-angle X-ray scattering measurements were effectively modeled by the form factor for a thin disk and gave a core thickness of approximately 10 nm. Dynamic light scattering measurements gave a distribution of hydrodynamic radii that was fully consistent with the dimensions inferred from microscopy and X-ray scattering. The unprecedented adoption of the flat disk morphology by a nonionic, coil−coil diblock copolymer is attributed to the extremely strong interfacial tension between the fluoropolymer core and the solvated hydrocarbon corona, as anticipated by superstrong segregation theory.

Introduction

The ability of amphiphilic molecules such as block copolymers, surfactants, and phospholipids to self-assemble into discrete micelles is well documented. Three canonical micellar morphologies are commonly encountered: spheres, cylindrical worms, and bilayer vesicles. The factors that dictate the selection of structure are also generally understood. In the case of block copolymers, for example, the three dominant considerations are the tension at the core/corona interface, the osmotic crowding of the well-solvated corona chains, and the stretching of the core blocks. Increasing interfacial tension drives the transitions from spheres to cylinders and then to bilayers, whereas increasing the corona block length reverses the sequence. Systematic progression through these three structures has been demonstrated in aqueous[1] and organic solvents[2−4] and mixtures thereof,[5−7] for example by variation of corona block length,[1,4−6] solvent quality,[2,4,6,7] and temperature.[3]

A different micellar morphology, that of the flat, circular disk, has also been anticipated theoretically, but only by accessing the so-called superstrong segregation limit (SSSL).[8] In this regime the interfacial tension γ becomes so large as to overwhelm the other free energy terms, leading to complete stretching of the core blocks and a flat interface; this is illustrated in Figure 1. Restriction of the flat sheets to finite size, i.e., circular disks rather than closing into vesicles, is favored due to corona chain crowding, as the edges of the disk provide relief of coronal congestion. Access to the SSSL requires remarkably large values of the interaction parameter between the core block and the solvated corona and thus is hard to achieve, especially in nonionic systems. In this paper we demonstrate the formation of flat disk micelles by self-assembly of diblock copolymers in an organic solvent. The core block is poly(hexafluoropropylene oxide), the corona block is 1,2-polybutadiene, and the solvent is bis(2-ethylhexyl) phthalate. This solvent is a glass-former, which facilitates imaging of the micelles by cryogenic transmission electron microscopy (cryo-TEM). A previous study of the micellization of these copolymers in toluene and chloroform

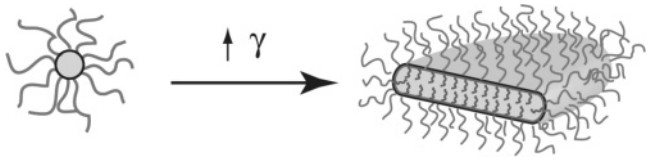

Figure 1. An illustration of the transition from a curved to a flat micelle interface as interfacial tension increases.

was suggestive of the formation of disk micelles, but in the absence of cryo-TEM images it was not possible to reach a definitive conclusion.[9]

Flat disk micelles have been reported in several other systems, but as far as we are aware never for a nonionic diblock copolymer comprising two random coil blocks. That is, one or more additional factor(s) have driven the selection of this unusual structure. For example, Nakano et al. demonstrated that disklike micelles could be formed upon crystallization of the core block; the crystallization into lamellae imposed an extended, thin sheet structure on the micellar core.[10] Rod−coil copolymers have also been shown to form disk micelles, in this case to meet the demands of close-packing the rodlike blocks.[11] This situation is analogous to the one considered here, in that the core chains adopt extended conformations. However, the crucial distinction is that in the rod−coil case the extended conformation is dictated by the rigidity of the rod block, whereas in our case, it is the strong interfacial tension that forces the core block to adopt a highly unfavorable extended conformation. Similarly, diblock copolymers in which one block is a polypeptide can form a variety of "noncanonical" structures due to the structure-directing effect of the α-helix[12] or β-sheet[13] motifs. Finally, the architecture of multiblock terpolymers has been exploited to induce disk formation. Our group demonstrated that ABC block terpolymers with poly(ethylene oxide), polystyrene, and fluorinated polybutadiene blocks formed core/shell/corona disk micelles with a typical radius (major axis) on the order of 50 nm.[14,15] Gomez et al. used an ABCA tetrablock copolymer, where the A blocks formed the corona, to produce layered sheetlike micelles.[16] Li et al. demonstrated that a charged ABC triblock copolymer forms disks in the presence of cationic diamines; they studied poly(acrylic acid)-*b*-poly(methyl acrylate)-*b*-polystyrene copolymers in a mixed solvent system of water

[†] Department of Chemical Engineering and Materials Science.
[‡] Department of Chemistry.
* Author for correspondence: e-mail lodge@chem.umn.edu.

10.1021/ma060633j CCC: $33.50
Published on Web 05/28/2006

and THF.[17] In each of these systems the multiple blocks increase the number of interfaces, thereby enhancing the importance of interfacial contributions to the overall free energy.[15]

Experimental Section

Samples and Solutions. The synthesis and characterization of 1,2-polybutadiene-*b*-poly(hexafluoropropylene oxide) (BF(6-6)) have been described in detail elsewhere;[9] the numerals denote the block molecular weights in kDa. Poly(hexafluoropropylene oxide) (PFPO) was provided by Dupont, which is commercially available as Krytox 157-FSH. PFPO was characterized by MALDI-TOF-MS; the M_n and PDI are 5.7 kDa and 1.1, respectively. From ^{1}H NMR spectroscopy and size exclusion chromatography, the M_n and PDI of 1,2-polybutadiene (1,2-PB) were determined to be 6.0 kDa and less than 1.1, respectively. The block copolymer BF(6-6) was synthesized through the coupling reaction of hydroxy-terminated 1,2-PB and acid-chloride-end-functionalized PFPO. Both blocks are atactic, noncrystallizing, flexible, low T_g materials.

Bis(2-ethylhexyl) phthalate (DEHP), a glass-forming solvent selective for 1,2-PB with $T_g \approx -85$ °C,[18] was purchased from Aldrich and used as received. BF(6-6) was directly dissolved in DEHP without the use of a cosolvent. The solutions were stirred at 70 °C for a minimum of 5 days and then cooled to room temperature. For microscopy and dynamic light scattering, the concentration of copolymer in solution was 1% (v/v). For small-angle X-ray scattering, the concentration was 3% (v/v). Measurements were also repeated after periods of several weeks and indicated no long-term evolution in micelle structure.

Cryogenic Transmission Electron Microscopy (Cryo-TEM). Cryo-TEM samples were prepared in a controlled environment vitrification system heated to 70 °C. Using a micropipet, an aliquot of the copolymer solution (~ 5 μL) was deposited onto a copper grid with a lacey, Formvar support film (Ted Pella, Inc., Product No. 01883). A thin film ca. 100 nm thick was deposited within the pores of the grid by using filter paper to remove excess sample. After waiting 90 s to allow for the relaxation of shear stresses induced during blotting, the grid was plunged into a reservoir of liquid nitrogen, thereby vitrifying the sample. For imaging, the prepared grids were transferred from liquid nitrogen and placed on the cryogenic sample holder (Gatan 626). A JEOL 1210 transmission electron microscope operating at 120 keV was used to view the samples. While imaging, the sample holder temperature was maintained at −178 °C. The images were captured digitally with a Gatan 724 multiscan CCD camera; the optical density gradients of the background were subtracted.

Dynamic Light Scattering. Using a 0.45 μm filter, 1 mL of a 1 vol % solution of BF(6-6) in DEHP was filtered into a dust-free glass tube (i.d. of 0.20 in., o.d. of 0.28 in.). The tube was sealed using paraffin film to prevent contamination from water vapor condensation and dust. Dynamic light scattering (DLS) was performed using a Lexel model 75 Ar ion laser with an operating wavelength of 488 nm. The scattered light intensity was detected using a Brookhaven photomultiplier tube and processed using a Brookhaven digital correlator (BI-9000AT). Intensity correlation functions $g^{(2)}(\tau)$ were measured over a range of wavevector values (q), and the data were fit using the following cumulant expression[19,20]

$$g^{(2)}(\tau) - 1 = \beta e^{(-2\bar{\Gamma}\tau)}(1 + \mu_2\tau^2/2!)^2 \quad (1)$$

where $\bar{\Gamma}$ is the first cumulant or average decay rate, μ_2 is the second cumulant, and the ratio $\mu_2/\bar{\Gamma}^2$ represents the mobility dispersity. The mean diffusion coefficient D_t was determined by a linear fit of the mean decay rate $\bar{\Gamma}$ vs q^2, with imposed zero intercept. Via the Stokes−Einstein relation, the effective hydrodynamic radius was determined as $R_h = k_BT/6\pi\eta D_t$. The viscosity of DEHP, 61 cP at 25 °C, was determined using a Rheometrics Fluids spectrometer (RFS-II) fitted with a Couette cell. The Laplace inversion routine CONTIN (version 2DP) was also used to analyze the size distribution of micelle dimensions.[21] CONTIN uses a regularization method to determine the $G(\Gamma)$ values that satisfy the following expression

$$g^{(1)}(\tau) = \int_0^\infty G(\Gamma)e^{-\Gamma\tau}\,d\Gamma \quad (2)$$

where $g^{(1)}(\tau)$ is the electric field correlation function and is related to the intensity correlation function by the Siegert relation.

Small-Angle X-ray Scattering (SAXS). The SAXS measurements were performed on beamline 5 ID-D, which is maintained by the DuPont-Northwestern-Dow Collaborative Access Team (DND-CAT) at the Advanced Photon Source of Argonne National Laboratory. For the reported measurements, the X-ray source was operated at 17 keV, and the wavelength was 0.73 Å. The sample-to-detector distance was 6.8 m, and the wavevector q was calibrated using a lab standard. The scattered intensities were measured using a Mar 165 mm CCD X-ray detector, which has a maximum resolution of 2048 × 2048 pixels with each pixel 78.75 μm square. Using the data reduction program FIT2D, the two-dimensional scattering profiles were integrated azimuthally to yield a one-dimensional plot of scattered intensity vs q.

BF(6-6) in DEHP solutions were loaded into quartz capillary tubes (Charles Supper Co., 2.0 mm o.d.). Scattering measurements were collected at room temperature, and the exposure time was varied between 20 and 60 s per sample. Data processing involved subtracting the scattered intensity of the solvent background from that of the block copolymer solutions. No attempt was made to convert the data to an absolute scale.

The scattering data were fit to a model expression to test the hypothesis that the block copolymers form disk micelles in solution. The general form factor expression for a block copolymer micelle is[22]

$$P(q) = A_{core}^2(q) + 2A_{core}(q)\,A_{corona}(q) + \left(\frac{Q-1}{Q}\right)A_{corona}^2(q) + Q(V\Delta\rho)_{corona}^2 P_{chain}(q) \quad (3)$$

where Q is the micelle aggregation number and $P_{chain}(q)$ is the form factor for a Gaussian coil, which is given by the Debye function, $2(e^{-q^2R_g^2} - 1 + q^2R_g^2)/q^4R_g^4$. The scattering contributions of the core and corona, A_{core} and A_{corona}, vary depending on the shape of the micelle. For an asymmetric disk, where the core thickness h_{core} is substantially smaller than the core radius R_{core}, these form factor amplitudes are[23]

$$A_{core} = Q(V\Delta\rho)_{core}\left[\frac{\sin(qh_{core}/2)}{qh_{core}/2}\right]P_{disk}^{1/2}(qR_{core}) \quad (4)$$

and

$$A_{corona} = Q(V\Delta\rho)_{corona}\psi(qR_g)\cos[q(h_{core}/2 + R_g)]P_{disk}^{1/2}(qR_{core}) \quad (5)$$

where $\Delta\rho$ is the excess scattering length density of the core ($\Delta\rho_{PFPO} = 6 \times 10^{-4}$ nm^{-2}) and corona ($\Delta\rho_{1,2-PB} = -7 \times 10^{-5}$ nm^{-2}) and V is the volume per chain of the core and corona ($V_{PFPO} = 5$ nm^3 and $V_{1,2-PB} = 11$ nm^3). The expressions $P_{disk}(x) = 2/x^2[1 - J_1(2x)/x]$ and $\psi(x) = (1 - e^{-x})/x$ are the form factor amplitudes for an infinitely thin disk and Gaussian chain, respectively. To achieve a better fit at the form factor minimum, a Gaussian distribution of thicknesses ranging from 7 to 12 nm with a standard deviation of 2 nm was used. In fitting the SAXS data, the adjustable model parameters were N, R_{core}, h_{core}, the standard deviation of the core thickness, and an arbitrary intensity scaling factor.

Results

Previously, the strong incompatibility between the diblock copolymer constituents, 1,2-PB and PFPO, was demonstrated.[9] When dissolved in certain selective solvents, DLS measurements

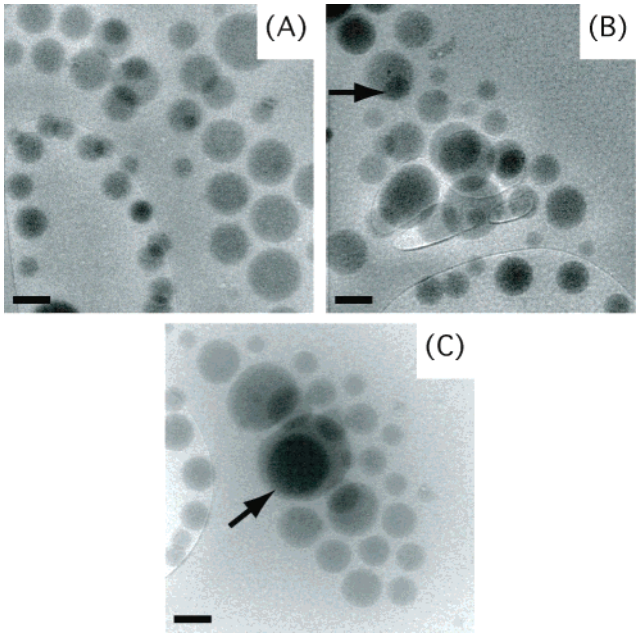

Figure 2. Cryo-TEM images of disk micelles formed from BF(6-6) copolymers in DEHP at 1 vol %. The scale bars represent 100 nm.

indicated that the BF diblocks form large, nonspherical micelles. For example, for 1 wt % solutions of BF(6-6) in toluene and chloroform, R_h was ca. 80 nm, which is significantly larger than the fully stretched length (FSL) of the chain, 35 nm. In the absence of conclusive microscopy evidence, we speculated that the copolymers formed coil−coil disk micelles in solution. In this paper, we present data that confirm this initial conjecture, albeit with a different solvent. Instead of chloroform or toluene as selective good solvents for 1,2-PB, we chose the glass former DEHP because it is better suited for cryo-TEM.

Cryo-TEM is the most direct technique for characterizing micelles in situ. Three representative images of the BF(6-6) micelles are shown in Figure 2. The electron densities of DEHP, 1,2-PB, and PFPO are 0.54, 0.50, and 0.92 mol e^-/cm^3, respectively.[24] On this basis the micelle core will appear darker than the solvent background. The electron density difference between DEHP and 1,2-PB is small, and thus the corona is not resolved in the cryo-TEM images. Figure 2 represents a large set of micelles with a broad distribution of sizes; core radii range from 20 to 100 nm. Assuming a planar zigzag conformation, the FSL of PFPO is 11 nm, which precludes the possibility that the imaged structures are "standard" spherical micelles. Furthermore, the micellar cores appear to have a uniform shading across their surface, implying a nearly constant thickness. The 100 nm scale bars in the figures are also approximate indicators of the confining film thickness. The flow of solution into the film, and the time allowed for relaxation, allow the anisometric micelles to find the preferred, "flat" orientation in the film, and thus no micelles are viewed "edge-on".

Interestingly, there are several examples of overlapping micelles in Figure 2; these are evidenced by the 50% reduction in transmitted electron intensity. The arrows in Figure 2 denote examples where one micelle lies completely on top of another. The propensity for these structures to stack up along the beam direction also suggests that their thickness is small relative to the core radius.

In an effort to gauge the profile thickness, the sample stage was tilted. If the micelles are disklike, tilting the sample stage should alter the two-dimensional projections, transforming them from circles to ellipses. Two images are presented in Figure 3. Image A is of a DEHP film with micelles lining the edge of the lacey support film, and image B is the result upon tilting the grid by 45°. Nearly all the micelles exhibit a distinct change in apparent shape upon tilting. However, it should be noted that the microscope employed is not equipped for precision tomography, and therefore this result should be considered supportive, rather than conclusive.

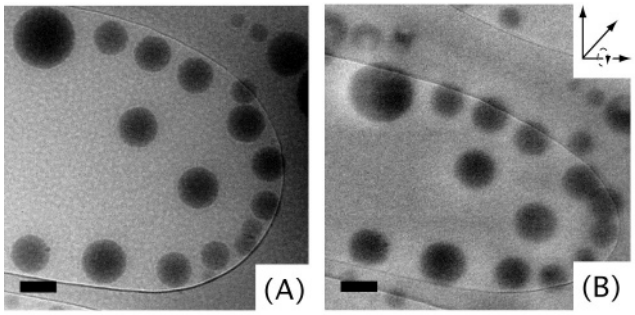

Figure 3. Comparison of a set of micelles with those imaged after tilting the sample stage 45°. The scale bars represent 100 nm.

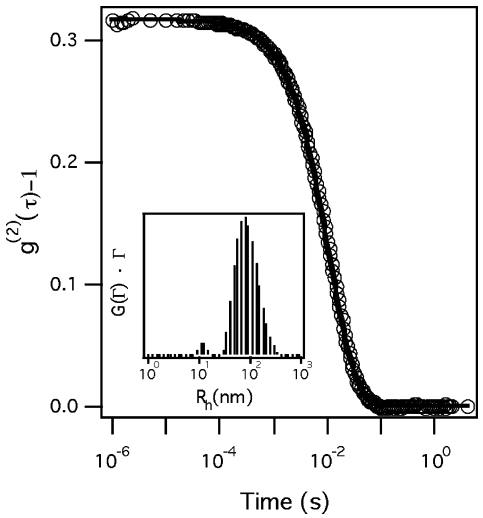

Figure 4. Intensity correlation function data at $\theta = 90°$ for a 1 vol % solution of BF(6-6) in DEHP at room temperature. The inset figure represents the size distribution based on a CONTIN inversion of the correlation function data.

Light and X-ray scattering are complementary experiments to microscopy. DLS provides a size estimate of the micelles in solution and a measure of the size distribution, $\mu_2/\bar{\Gamma}^2$. A typical intensity correlation function is illustrated in Figure 4 at $\theta = 90°$ and room temperature. From data collected at a series of angles, the average $R_h = 60$ nm. At $\theta = 90°$, the size dispersity is 0.31, which is broad compared to the typical value for a solution of block copolymer spherical micelles ($\mu_2/\bar{\Gamma}^2 < 0.1$). The distribution determined using CONTIN is shown as an inset in Figure 4. The majority of the micelles are centered at an R_h just below 100 nm. A double-exponential fit to the correlation function was not successful, and therefore we are inclined to discount the small peak at 10 nm. Thus, a single, broad distribution of micellar sizes (R_h) ranging from 20 to 150 nm describes the system, in good agreement with the cryo-TEM images. These results are also similar to those reported previously, where the mean R_h was 80 nm in toluene and 78 nm in chloroform.

SAXS measurements facilitate determination of the disk core thickness h_{core}. The scattered intensity for a 3 vol % solution of BF(6-6) micelles in DEHP is given in Figure 5. The roots of

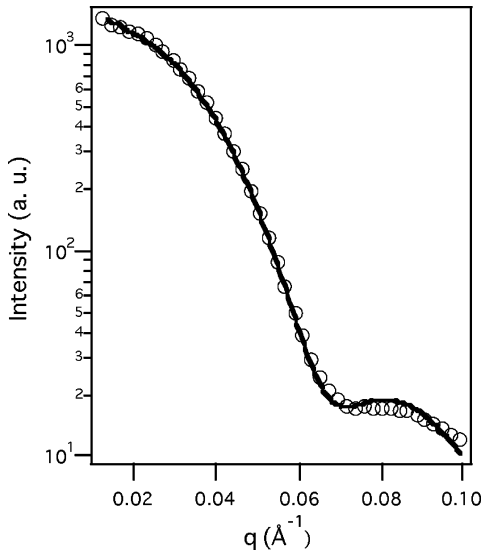

Figure 5. Synchrotron SAXS data for a 3 vol % solution of BF(6-6) copolymer in DEHP. The solid line represents a fit of the data using the form factor expression for disk micelles proposed by Pedersen.[23]

Table 1. Comparison of the Micelle Hydrodynamic Radius Measured by DLS to That Calculated for a Disk Micelle Using the Core Radius and Thickness Determined by Microscopy and SAXS

	fully stretched length[a] (nm)	$R_{g,1,2-PB}$ (nm)	$\langle R_{core}\rangle_z$[b] (nm)	h_{core}[c] (nm)	$\langle R_h\rangle$[d] (nm)	R_h[e] (nm)
BF(6-6)	35	3	80	9	58	60

[a] Calculated assuming a planar, zigzag conformation. [b] *Z*-average core radius for 140 particles. [c] Disk thickness from a form factor fit of SAXS data. [d] Hydrodynamic radius given by eq 6 for an ensemble of particles characterized by cryo-TEM and SAXS. [e] DLS result.

the form factor expression for the micelle core (eq 4) provide a reasonable estimate of the thickness h_{core}. In Figure 5, the scattered intensity minimum occurs at a q value of 0.07 Å^{-1}, which corresponds to a thickness of 8.7 nm. Using eqs 3−5 to fit the data, the resulting disk thickness is 9.1 nm; the fit is shown as a solid line in Figure 5.

Discussion

Each of the three experiments provides complementary information. If BF(6-6) diblocks form disk micelles in solution, these results should be internally self-consistent. Experimentally, the micelle hydrodynamic radius (DLS), core radius (cryo-TEM), and thickness (SAXS) are known; these results are summarized in Table 1. The reported core radius is a *z*-average based on an ensemble of 140 particles. For a disk micelle, the dependence of R_h on the radius and thickness is given by[25]

$$R_h = \frac{3}{2}R\left(\alpha + \frac{2R}{h}\ln\left(\frac{h}{2R} + \alpha\right) - \frac{h}{2R}\right)^{-1} \qquad (6)$$

where $\alpha = \sqrt{1+(h/2R)^2}$, $R \cong R_{core} + 2R_{g,1,2-PB}$, and $h \cong h_{core} + 4R_{g,1,2-PB}$. For each of the measured particles, R_h was calculated by eq 6, and then the values were weighted to determine a DLS-equivalent, harmonic average, $\langle R_h\rangle^{-1} = \sum(V^2/R_h)/\sum V^2$, where V is the solid particle volume, $\pi R^2 h$. The two measures of hydrodynamic radius are within experimental error of one another, and thus the SAXS, cryo-TEM, and DLS data are fully consistent with the formation of coil−coil diblock copolymer disk micelles.

It is worth considering whether the micelles could be vesicles, rather than disks. For example, the SAXS data in Figure 5 could

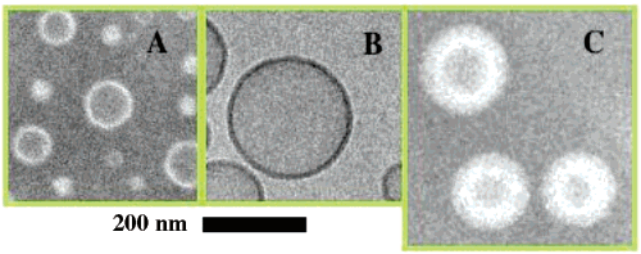

Figure 6. Cryo-TEM images of vesicles formed from (A) polybutadiene-*b*-poly(ethylene oxide) in [bmim$^+$][PF_6^-],[26] (B) polystyrene-*b*-poly(dimethylsiloxane) in diethyl phthalate,[27] and (C) polystyrene-*b*-polyisoprene in dimethyl and diethyl phthalate.[2]

be equally well described with a vesicle form factor.[23] However, the microscopy images in Figures 2 and 3 show no hint of the distinct "lip" that is characteristic of cryo-TEM images of vesicles. To underscore this difference, in Figure 6 we present cryo-TEM images obtained in the same manner, and on the same equipment, of vesicles formed in three different block copolymer/solvent systems, all of which show such a lip. Specifically, images A, B, and C of Figure 6 show vesicles from polybutadiene-*b*-poly(ethylene oxide) in the ionic liquid [bmim$^+$][PF_6^-],[26] polystyrene-*b*-poly(dimethylsiloxane) in diethyl phthalate,[27] and polystyrene-*b*-polyisoprene in a mixture of dimethyl and diethyl phthalate,[2] respectively. Despite the variety of systems, and the "reverse" contrast in panels A and C, the vesicle morphology is clearly revealed in all cases. Given that panels B and C correspond to dialkyl phthalate solvents in particular, these images are a strong argument against vesicles for the system considered here.

Another possibility to consider is that the micelles are oblate ellipsoids, rather than thin, flat disks. However, attempts to model the SAXS data in this way were far less successful. In particular, the presence of a distinct minimum in the form factor appears to require a well-defined micellar thickness, rather than a smoothly varying one.

We now consider whether the formation of disk micelles is completely consistent with expectation based on the SSSL. Previously, the Flory−Huggins parameter χ for BF(6-6) was estimated to be 4 based on the application of mean-field theory to the cylindrical domain spacing of the bulk copolymer.[9,28] Thus, these experiments are at least qualitatively consistent with the theory, in that disk micelles are anticipated when the interfacial tension becomes extremely high. Semenov et al. suggested the criterion for accessing the SSSL is that $\gamma \sim N_{core}b_{core}^{5/2}/\upsilon_{core}^{3/2}$.[8] In our case, N_{core} is 35, the statistical segment length for the core block b_{core} is 3.9 Å,[29,30] and the monomeric volume of the core block υ_{core} is 145 Å^3. Given that $\gamma \sim \sqrt{\chi}b^{-2}$, the SSSL is attained for $\sqrt{\chi}$ values on the order of 10. Based solely on the bulk Flory−Huggins parameter, our system fails to satisfy this criterion. However, the contribution of the solvent−core block interaction to γ will be significant and may account for the discrepancy. Another factor to consider is the role of conformational asymmetry, as this can shift the phase boundaries between block copolymer morphologies markedly.[31,32] For the BF(6-6) copolymer the asymmetry factor is 1.8, which indicates that there is an increased preference for lamellae over morphologies with curved interfaces.[33] This tendency coupled with the previous arguments provides a physical explanation for the observed formation of coil−coil disk micelles.

Another micellar characteristic anticipated by the SSSL theory is that the disk thickness should be essentially twice the fully stretched length of the core block.[8] The FSL of PFPO is 11

nm, thus the disk thickness should be of order 20 nm. The fitted value from SAXS is significantly lower than this, which suggests that either the core blocks are not so fully stretched or that the blocks are interdigitated.[34]

Summary

A combination of cryo-TEM, dynamic light scattering, and small-angle X-ray scattering provides definitive evidence of flat disk micelles for a 1,2-polybutadiene−poly(hexafluoropropylene oxide) diblock copolymer dissolved in a good solvent for the hydrocarbon block. As far as we are aware, this is the first example of a coil−coil, nonionic diblock copolymer adopting such a morphology. This structure is clearly the result of an unusually large interfacial tension between the fluoropolymer and the solvated polybutadiene. The observation of flat disk micelles is at least qualitatively consistent with expectation based on the superstrong segregation limit.

Acknowledgment. This work was supported by the MRSEC Program of the National Science Foundation under Award DMR-0212302. W. F. Edmonds thanks 3M for their support through the 3M Graduate Science and Technology Fellowship. Portions of this work were performed at the DuPont-Northwestern-Dow Collaborative Access Team (DND-CAT) Synchrotron Research Center located at Sector 5 of the Advanced Photon Source. DND-CAT is supported by the E.I. DuPont de Nemours & Co., The Dow Chemical Company, the U.S. National Science Foundation through Grant DMR-9304725, and the State of Illinois through the Department of Commerce and the Board of Higher Education Grant IBHE HECA NWU 96. Use of the Advanced Photon Source was supported by the U.S. Department of Energy, Basic Energy Sciences, Office of Energy Research under Contract W-31-102-Eng-38.

References and Notes

(1) Jain, S.; Bates, F. S. *Science* **2003**, *300*, 460.
(2) Bang, J.; Jain, S.; Li, Z.; Lodge, T. P.; Pedersen, J. S.; Kesselman, E.; Talmon, Y. *Macromolecules* **2006**, *39*, 1199.
(3) LaRue, I.; Adam, M.; Pitsikalis, M.; Hadjichristidis, N.; Rubinstein, M.; Sheiko, S. S. *Macromolecules* **2006**, *39*, 309.
(4) Ding, J.; Liu, G.; Yang, M. *Polymer* **1997**, *38*, 5497.
(5) Zhang, L.; Eisenberg, A. *Science* **1995**, *268*, 1728.
(6) Shen, H.; Eisenberg, A. *Macromolecules* **2000**, *33*, 2561.
(7) Shen, H.; Eisenberg, A. *J. Phys. Chem. B* **1999**, *103*, 9473.
(8) Semenov, A. N.; Nyrkova, I. A.; Khokhlov, A. R. *Macromolecules* **1995**, *28*, 7491.
(9) Zhu, S.; Edmonds, W. F.; Hillmyer, M. A.; Lodge, T. P. *J. Polym. Sci., Part B: Polym. Phys.* **2005**, *43*, 3685.
(10) Nakano, M.; Matsumoto, K.; Matsuoka, H.; Yamaoka, H. *Macromolecules* **1999**, *32*, 4023.
(11) Wu, J.; Pearce, E. M.; Kwei, T. K.; Lefebvre, A. A.; Balsara, N. P. *Macromolecules* **2002**, *35*, 1791.
(12) Vandermeulen, G. W. M.; Tziatzios, C.; Klok, H. A. *Macromolecules* **2003**, *36*, 4107.
(13) Burkoth, T. S.; Benzinger, T. L. S.; Jones, D. N. M.; Hallenga, K.; Meredith, S. C.; Lynn, D. G. *J. Am. Chem. Soc.* **1998**, *120*, 7655.
(14) Zhou, Z.; Li, Z.; Ren, Y.; Hillmyer, M. A.; Lodge, T. P. *J. Am. Chem. Soc.* **2003**, *125*, 10182.
(15) Lodge, T. P.; Hillmyer, M. A.; Zhou, Z.; Talmon, Y. *Macromolecules* **2004**, *37*, 6680.
(16) Gomez, E. D.; Rappl, T. J.; Agarwal, V.; Bose, A.; Schmutz, M.; Marques, C. M.; Balsara, N. P. *Macromolecules* **2005**, *38*, 3567.
(17) Li, Z.; Chen, Z.; Cui, H.; Hales, K.; Qi, K.; Wooley, K. L.; Pochan, D. J. *Langmuir* **2005**, *21*, 7533.
(18) Savin, D. A.; Larson, A. M.; Lodge, T. P. *J. Polym. Sci., Part B: Polym. Phys.* **2004**, *42*, 1155.
(19) Koppel, D. E. *J. Chem. Phys.* **1972**, *57*, 4814.
(20) Frisken, B. J. *Appl. Opt.* **2001**, *40*, 4087.
(21) Provencher, S. W. *Comput. Phys. Commun.* **1982**, *27*, 213.
(22) Pedersen, J. S.; Gerstenberg, M. C. *Macromolecules* **1996**, *29*, 1363.
(23) Pedersen, J. S. *J. Appl. Crystallogr.* **2000**, *33*, 637.
(24) Determined using bulk densities of 0.985 g/cm^3 (DEHP), 0.9 g/cm^3 (1,2-PBD), and 1.9 g/cm^3 (PFPO).
(25) Mazer, N. A.; Benedek, G. B.; Carey, M. C. *Biochemistry* **1980**, *19*, 601.
(26) He, Y.; Li, Z.; Simone, P.; Lodge, T. P. *J. Am. Chem. Soc.* **2006**, *128*, 2745.
(27) Abbas, S.; Li, Z.; Lodge, T. P., University of Minnesota, unpublished results.
(28) For this calculation, N is based on a common reference volume of 114 Å^3.
(29) Cantow, M. J. R.; Larrabee, R. B.; Barrall, E. M., II; Butner, R. S.; Cotts, P.; Levy, F.; Ting, T. Y. *Makromol. Chem.* **1986**, *187*, 2475.
(30) Hamada, T. *Phys. Chem. Chem. Phys.* **2000**, *2*, 115.
(31) Vavasour, J. D.; Whitmore, M. D. *Macromolecules* **1993**, *26*, 7070.
(32) Matsen, M. W.; Schick, M. *Macromolecules* **1994**, *27*, 4014.
(33) Matsen, M. W.; Bates, F. S. *J. Polym. Sci., Part B: Polym. Phys.* **1997**, *35*, 945.
(34) Battaglia, G.; Ryan, A. J. *J. Am. Chem. Soc.* **2005**, *127*, 8757.

MA060633J